

Fluid-dynamical approach to collective modes in metal clusters

João da Providência, Jr. and Raphael de Haro, Jr.*

Departamento de Física, Universidade de Coimbra, P-3000 Coimbra, Portugal

(Received 20 April 1993)

A simple variational method has recently been used to obtain the bulk-plasmon dispersion relation in a metal. In the present work we investigate the eigenmodes of the valence electrons in a metal cluster considering a semiclassical version of the method presented by Andō and Nishizaki. As a variational function we consider the Slater determinant $|\phi\rangle$ which is related to the Slater determinant $|\phi_0\rangle$, describing the ground state, by means of the unitary transformation $|\phi\rangle = e^{(i/\hbar)S}|\phi_0\rangle$, where $S(\mathbf{x}, \mathbf{p}, t) = \chi(\mathbf{x}, t) + \frac{1}{2}[\mathbf{p} \cdot \mathbf{s}(\mathbf{x}, t) + \mathbf{s}(\mathbf{x}, t) \cdot \mathbf{p}]$. We use a polynomial approximation to determine the dynamical fields $\chi(\mathbf{x}, t)$ and $\mathbf{s}(\mathbf{x}, t)$. It is shown that the eigensolutions satisfy the energy weighted sum rule and the cubic energy weighted sum rule. The spectrum of excited energies, as well as transition densities and currents are obtained for the sodium, aluminum, and silver.

I. INTRODUCTION

The physical properties of metal particles of small dimensions (metal clusters) is presently the object of intensive studies, both theoretical and experimental.¹⁻³

Semiclassical methods appear as a possible alternative to study the properties of heavy nuclei,⁴⁻¹⁵ (clusters of nucleons) and their use has proved to be particularly fruitful in this area.

These methods are rather intuitive, and have a great physical appeal since they describe the collective motion in terms of physically meaningful quantities such as the current, density, and pressure tensor. These quantities are related to the distribution function f in (\mathbf{x}, \mathbf{p}) space. The calculations involved in solving the semiclassical problem have the advantage of being simpler than a full quantum-mechanical calculation. The numerical effort involved in these calculations does not depend on the number of atoms of the metal cluster, which is not the case for a completely quantum-mechanical calculation such as the one developed by Ekardt.¹⁶ Calculations for Na_{338} have recently been reported.¹⁷ However, it appears that quantal calculations very soon become prohibitive if the number of atoms is further increased.

We propose to apply such semiclassical methods to study the collective modes of the electron plasma in metal clusters. It is particularly interesting to evaluate the energies of the collective multipole surface excitations of metal clusters.

Instead of solving the exact semiclassical random-phase approximation (RPA) equations, it is convenient to consider a related variational scheme in terms of some collective variables which parametrize the fluctuations of the distribution function. Following these ideas, we would like to consider a variational scheme analogous to the one considered by Andō and Nishizaki⁴ where one deals with a variational field χ which may be interpreted as the velocity potential, and a scaling field \mathbf{s} which is related to the transition density.

In a recent paper⁵ a simple variational approach⁴ was proposed to derive the bulk-plasmon dispersion relation

in a metal. Our present purpose is to apply a semiclassical version of the variational method described in Ref. 4 to the calculation of the eigenmodes of valence electrons in a metal cluster.

II. THE EQUILIBRIUM STATE

The operator $H = T + V$ stands for the Hamiltonian of an electron gas in a uniform positive background (jellium model), and T and V , respectively, are,

$$T = \sum_{j=1}^N \frac{p_j^2}{2m}, \tag{1}$$

$$V = \sum_{i < j} \frac{e^2}{|\mathbf{x}_i - \mathbf{x}_j|} + \sum_{j=1}^N U(\mathbf{x}_j) + W, \tag{2}$$

where $U(\mathbf{x})$ is the potential energy due to the uniform positive density distribution, and W is the electrostatic energy of the positive background ($-e$ being the electron charge).

In the equilibrium state the density of the jellium, $n_0(\mathbf{x}) = n_0(0)\Theta(R - r)$, coincides with the density of the valence electrons. We are considering a metal cluster with a spherical shape. The constants $n_0(0)$ and R , associated with the cluster, deserve some attention. In particular we have $N = 4\pi n_0(0)R^3/3$, where N stands for the number of valence electrons. In order to solve the equilibrium problem, we minimize the energy. The energy of the valence electrons is obtained by adding the kinetic energy of the valence electrons to their potential energy. The energy due to the interaction between the valence electrons themselves, and that due to the interaction of the valence electrons with the jellium, both contribute to the potential energy.

We assume that the electron dynamics is well approximated by the Vlasov equation.¹⁵ Since Vlasov dynamics neglects exchange effects and electron-electron correlations, due to its classical nature, these effects are taken into account phenomenologically by adding a two-body δ interaction (exchange effects) and a three-body δ interaction (correlation effects) to the Hamiltonian. We also add

a one-body δ interaction which describes the effect of the more conventional pseudopotential. The effective energy functional referring to the metal cluster may therefore be expressed as follows:

$$E = \int d\Gamma f \left[\frac{p^2}{2m} + a_1 \right] + \frac{1}{2} \int d\Gamma_1 \int d\Gamma_2 v_{12} f(1) f(2) \\ + \frac{1}{3!} \int d\Gamma_1 \int d\Gamma_2 \int d\Gamma_3 v_{123} f(1) f(2) f(3) \\ + E_{e-j}^{(c)} + W. \quad (3)$$

The term $E_{e-j}^{(c)}$ stands for the energy associated with the Coulomb interaction electron-jellium,

$$E_{e-j}^{(c)} = -e^2 \int d^3x_1 \int d^3x_2 \frac{n(1)n_0(2)}{|\mathbf{x}_1 - \mathbf{x}_2|}, \quad (4)$$

and W stands for the interaction of the jellium with itself;

$$W = \frac{e^2}{2} \int d^3x_1 \int d^3x_2 \frac{n_0(1)n_0(2)}{|\mathbf{x}_1 - \mathbf{x}_2|}. \quad (5)$$

The symbol f stands for the distribution function of the valence electrons, n is the density of the valence electrons, $d\Gamma = g d^3x d^3p / (2\pi\hbar)^3$ is the volume element in phase space, and $g=2$ is the spin multiplicity.

We follow a phenomenological procedure, introducing an effective interaction (Skyrme interaction) which contains two- and three-body terms. We adjust the parameters of this interaction in order to obtain the experimental values of the density, energy, and bulk modulus of an homogeneous system. These interactions lead to the appearance of an effective potential energy of the form $V_{\text{eff}} = \int d^3x \sum_{\sigma=1}^3 a_{\sigma} n^{\sigma}$, which is obtained from the one-body δ interaction [$a_1 = b \int d^3x' n_0(\mathbf{x}) \delta(\mathbf{x} - \mathbf{x}')$] and from the effective interactions $v'_{12} = c \delta(\mathbf{x}_1 - \mathbf{x}_2)$ and $v_{123} = d \delta(\mathbf{x}_1 - \mathbf{x}_2) \delta(\mathbf{x}_2 - \mathbf{x}_3)$. To the two-body interaction v'_{12} , we add the Coulomb interaction, so that finally we work with a two-body effective interaction, $v_{12} = c \delta(\mathbf{x}_1 - \mathbf{x}_2) + (e^2/|\mathbf{x}_1 - \mathbf{x}_2|)$. Therefore, in Eq. (3) the term in v_{12} includes the energy associated with the electron-electron Coulomb interaction $E_{e-e}^{(c)}$:

$$E_{e-e}^{(c)} = \frac{e^2}{2} \int d^3x_1 \int d^3x_2 \frac{n(1)n(2)}{|\mathbf{x}_1 - \mathbf{x}_2|}. \quad (6)$$

In the energy functional we are neglecting terms which imply derivatives of the density of the free electrons. We also restrict the electron density to be homogeneous when determining the equilibrium properties. This assumption is consistent with our basic approximation. Such an approach has been used in the context of nuclear physics, and it has been shown^{11,13} that it gives good results when compared to one that includes terms with derivatives of the density in the energy functional, and therefore is associated with a smooth surface profile of the nucleus. We are therefore considering a semiclassical approximation, in the sense that we are not including quantum corrections related to the so-called gradient terms associated with derivatives of the density n in the energy functional E . The expression for the energy in the equilibrium state

is then

$$E = \Omega \left[\tau + \sum_{\sigma=1}^3 a_{\sigma} n^{\sigma} \right], \quad (7)$$

where $\Omega = N/n$ stands for the volume of the cluster. We note that the Coulomb energy does not contribute to the total energy, since there is a cancellation of the potential-energy contributions of the jellium and the valence electrons. Here τ is the kinetic-energy density;

$$\tau = g \int \frac{d^3p}{(2\pi\hbar)^3} f \frac{p^2}{2m} = \frac{4\pi}{(2\pi\hbar)^3} \frac{p_F^5}{5m}. \quad (8)$$

The equilibrium distribution function of the gas of valence electrons is

$$f(\mathbf{x}, \mathbf{p}) = \Theta \left[\lambda - \frac{p^2}{2m} - U \right] \Theta(R - r), \quad (9)$$

where U is the self-consistent potential;

$$U(1) = a_1 + \int d\Gamma_2 v_{12} f(2) \\ + \frac{1}{2} \int d\Gamma_2 \int d\Gamma_3 v_{123} f(2) f(3) \\ - \int d^3x_2 \frac{e^2}{|\mathbf{x}_1 - \mathbf{x}_2|} n_0(2). \quad (10)$$

In the equilibrium state there is also a cancellation of the electrostatic contribution of the jellium and of the valence electrons to the self-consistent potential, so that we have $U = \sum_{\sigma=1}^3 a_{\sigma} \sigma n^{\sigma-1}$.

The total energy may be expressed in terms of the electron density n :

$$E = \frac{N}{n} \left[\frac{3\hbar^2}{10m} (3\pi^2)^{2/3} n^{5/3} + \sum_{\sigma} a_{\sigma} n^{\sigma} \right]. \quad (11)$$

The equilibrium density is obtained by requiring that E should be minimal with respect to the variation of the density,

$$\delta E = \delta n N \left[\frac{\hbar^2}{5m} (3\pi^2)^{2/3} n^{-1/3} + \sum_{\sigma} a_{\sigma} (\sigma - 1) n^{\sigma-2} \right] \\ = 0. \quad (12)$$

Thus the equilibrium condition may be expressed as

$$\frac{2\tau_0}{3} + \sum_{\sigma} a_{\sigma} (\sigma - 1) n_0^{\sigma} = 0. \quad (13)$$

In our case, in the equilibrium state, the particle density n_0 and the kinetic-energy density τ_0 are step functions of r .

III. LAGRANGIAN AND EQUATIONS OF MOTION

We begin by considering a general quantum-mechanical Lagrangian given by

$$L = i\hbar \langle \phi | \dot{\phi} \rangle - \langle \phi | H | \phi \rangle, \quad (14)$$

and a variational function chosen to be the Slater determinant $|\phi\rangle$ which is related to the Slater determinant

$|\phi_0\rangle$, describing the ground state, by means of the unitary transformation

$$|\phi\rangle = \exp\left[\frac{i}{\hbar}\hat{S}\right]|\phi_0\rangle, \quad (15)$$

where \hat{S} is a Hermitian one-body operator. For small amplitude deviations from the equilibrium state, one obtains the following harmonic Lagrangian:

$$L^{(2)} = \frac{i}{2\hbar} \langle \phi_0 | [\hat{S}, \dot{\hat{S}}] | \phi_0 \rangle - \frac{1}{2\hbar^2} \langle \phi_0 | [\hat{S}, [H, \hat{S}]] | \phi_0 \rangle. \quad (16)$$

We consider the classical limit of Lagrangian (16), retaining only the leading terms in a Wigner-Kirkwood expansion in powers of \hbar .

As in Refs. 4 and 7, we will restrict the generator \hat{S} to the first two terms in an expansion in powers of the momentum. We write

$$\hat{S} = \sum_{j=1}^N S(\mathbf{x}_j, \mathbf{p}_j, t), \quad (17)$$

$$S(\mathbf{x}, \mathbf{p}, t) = \chi(\mathbf{x}, t) + \frac{1}{2}[\mathbf{p} \cdot \mathbf{s}(\mathbf{x}, t) + \mathbf{s}(\mathbf{x}, t) \cdot \mathbf{p}], \quad (18)$$

where χ and \mathbf{s} are taken as basic dynamical variables.

We then obtain, from the quantal Lagrangian (16), the following semiclassical Lagrangian:

$$L^{(2)} = \int d^3x \frac{n_0}{2} (\mathbf{s} \cdot \nabla \dot{\chi} - \dot{\mathbf{s}} \cdot \nabla \chi) - T^{(2)}[\chi] - E^{(2)}[\mathbf{s}], \quad (19)$$

where

$$T^{(2)}[\chi] = \int d^3x \frac{n_0}{2m} (\nabla \chi) \cdot (\nabla \chi), \quad (20)$$

$$E^{(2)}[\mathbf{s}] = \int d^3x \left[\frac{\tau_0}{3} [(\nabla \cdot \mathbf{s})^2 + \frac{1}{2}(\partial_\alpha s_\beta + \partial_\beta s_\alpha)^2] + \sum_\sigma a_\sigma \frac{\sigma(\sigma-1)}{2} n_0^\sigma (\nabla \cdot \mathbf{s})^2 \right] + \frac{e^2}{2} \int d^3x_1 d^3x_2 \frac{[\nabla \cdot (n_0 \mathbf{s})]_1 [\nabla \cdot (n_0 \mathbf{s})]_2}{|\mathbf{x}_1 - \mathbf{x}_2|}. \quad (21)$$

It has been possible to obtain Eq. (21) due to the cancellation of the electron-jellium contribution with part of the electron-electron contribution. In order to clarify this

$$\nabla \cdot (n_0 \mathbf{s}) = n_0(0) \sum_{k=k_{\min}}^{k_{\max}} \frac{b_k}{R^k} \{ -\delta(R-r) k r^{k-1} Y_{l0} + \Theta(R-r) [k(k+1) - l(l+1)] r^{k-2} Y_{l0} \}, \quad (26)$$

and

$$\mathbf{j} = \frac{n_0}{m} \sum_{k=k_{\min}}^{k_{\max}} \frac{a_k}{R^k} (k r^{k-2} \mathbf{x} Y_{l0} + r^k \nabla Y_{l0}). \quad (27)$$

Since the transition density $\delta n = \nabla \cdot (n_0 \mathbf{s})$ should not diverge at the origin, it follows from Eq. (26) that k_{\min} should not be less than 2, except for $l=1$, when it should not be less than 1.

Inserting expressions (24) and (25) into Eqs. (19)–(21), we obtain the Lagrangian

point we consider the electron-jellium and electron-electron electrostatic energies $E_{e-j}^{(c)}$ and $E_{e-e}^{(c)}$, respectively, given by Eqs. (4) and (6), and insert the expression $n_0 + \nabla \cdot (n_0 \mathbf{s}) + \frac{1}{2} \partial_\mu (s_\mu \partial_\nu (n_0 s_\nu))$ in place of n . This quantity represents, up to second order, the density of the valence electrons. Adding these two integrals, and assuming that we have a neutral cluster, it is then clear that the Coulomb contribution to the energy functional $E^{(2)}[s]$ reduces to the last integral in Eq. (21).

The distribution function $f(\mathbf{r}, \mathbf{p}, t)$ is related to the equilibrium distribution function f_0 by means of the canonical transformation (classical counterpart of a unitary transformation): $f = f_0 + \{f_0, S\} + \frac{1}{2} \{ \{f_0, S\}, S \} + \dots$, where the curly brackets $\{ \}$ stand for the Poisson brackets, and S stands for the Wigner transform of the generator \hat{S} . The density is obtained by integrating the distribution function f in momentum space, and the current is obtained by integrating in momentum space the distribution function f multiplied by \mathbf{p}/m . Up to first order in the variational fields χ and \mathbf{s} , one has

$$n = g \int \frac{d^3p}{(2\pi\hbar)^3} f = n_0 + \nabla \cdot (n_0 \mathbf{s}), \quad (22)$$

and

$$\mathbf{j} = g \int \frac{d^3p}{(2\pi\hbar)^3} f \frac{\mathbf{p}}{m} = \frac{n_0}{m} \nabla \chi. \quad (23)$$

The field $\chi(\mathbf{x}, t)$ plays the role of the velocity potential, while $\mathbf{s}(\mathbf{x}, t)$ may be interpreted as the displacement field in continuum mechanics.

Following the method of Ref. 14, we make an expansion of the dynamical fields χ and \mathbf{s} in multipoles and, for each multipolarity, we express the radial dependence by a polynomial in (r/R) :

$$\mathbf{s} = \nabla \left[\sum_{k=k_{\min}}^{k_{\max}} b_k(t) (r/R)^k Y_{l0} \right], \quad (24)$$

$$\chi = \sum_{k=k_{\min}}^{k_{\max}} a_k(t) (r/R)^k Y_{l0}, \quad (25)$$

where the variables $a_k(t)$ and $b_k(t)$ are fixed variationally by requiring that the action integral be stationary. Inserting expressions (24) and (25) into Eqs. (22) and (23), we find

$$L^{(2)} = \frac{1}{2} \sum_{kq} \left\{ A_{kq} \left[(b_k \dot{a}_q - \dot{b}_k a_q) - \frac{1}{m} a_k a_q \right] - B_{kq} b_k b_q \right\}. \quad (28)$$

Here, and in the following equations, the dots over the

dynamical fields stand for a time derivative. Moreover,

$$T^{(2)}[\chi] = \frac{1}{2m} \sum_{kq} A_{kq} a_k a_q, \quad (29)$$

$$E^{(2)}[\mathbf{s}] = \frac{1}{2} \sum_{kq} B_{kq} b_k b_q, \quad (30)$$

where

$$A_{kq} = n_0(0)R \frac{kq + l(l+1)}{k+q+1} \quad (31)$$

and

$$B_{kq} = \frac{2}{(k+q-1)R} \left\{ \frac{2\tau_0(0)}{3} \{ [l(l+1)]^2 + l(l+1)(2kq - 3k - 3q + 1) \right. \\ \left. + kq(kq - k - q + 3) \right\} + \left[\frac{\mathcal{B}}{2} - \frac{2\tau_0(0)}{9} \right] [k(k+1) - l(l+1)][q(q+1) - l(l+1)] \\ + \frac{n_0(0)m\omega_p^2 R}{k+q+1} \left[kq + \frac{l(l+1)(2l-k-q)}{(2l+1)} \right]. \quad (32)$$

Here

$$\omega_p^2 = \frac{4\pi n_0(0)e^2}{m} \quad (33)$$

is the plasma frequency or bulk volume plasmon, and the coefficient \mathcal{B} is the compression modulus calculated in the equilibrium state,

$$\mathcal{B} = -V \frac{\partial P}{\partial V} \left[\equiv n^2 \frac{\partial^2 (E/\Omega)}{\partial n^2} \right]. \quad (34)$$

The action integral should be stationary for arbitrary variations of the coefficients a_q ,

$$\delta I = - \int dt \sum_{kq} \delta a_q A_{qk} \left[\dot{b}_k + \frac{1}{m} a_k \right] = 0, \quad (35)$$

and for arbitrary variations of the coefficients b_q ,

$$\delta I = \int dt \sum_{kq} \delta b_q (A_{qk} \dot{a}_k - B_{kq} b_k) = 0. \quad (36)$$

Requiring the action integral to be stationary for arbitrary variations of the variables a_q and b_q , the following equations are obtained:

$$\sum_k A_{qk} \left[\dot{b}_k + \frac{a_k}{m} \right] = 0 \quad (37)$$

and

$$\sum_k (A_{qk} \dot{a}_k - B_{kq} b_k) = 0. \quad (38)$$

Since the matrix A_{kq} is nonsingular, it follows that

$$\dot{b}_k + \frac{a_k}{m} = 0. \quad (39)$$

We note from Eq. (39) that we easily obtain the continuity equation:

$$\nabla \cdot (n_0 \dot{\mathbf{s}}^{(j)}) + \nabla \cdot \left[\frac{n_0}{m} \nabla \chi^{(j)} \right] = 0. \quad (40)$$

From Eqs. (37) and (38), we find the following matrix equation for the variables b_k :

$$-m \sum_k A_{qk} \ddot{b}_k = \sum_k B_{kq} b_k. \quad (41)$$

We assume harmonic time dependence for the variables a_k and b_k ($\ddot{b}_k = -\omega^2 b_k$), so that, from Eq. (41), we obtain the following eigenvalue equation:

$$\omega^2 m \sum_k A_{qk} b_k = \sum_k B_{kq} b_k. \quad (42)$$

Solving the eigenvalue Eq. (42), we obtain the normal modes for each value of l , which are characterized by the eigenfrequencies ω_j and the eigenvectors $(\chi^{(j)}, \mathbf{s}^{(j)})$. In particular, if we choose a variational scheme of order $k_{\text{dim}} = k_{\text{max}} - k_{\text{min}} + 1$, we obtain k_{dim} eigenmodes. As we will see in Sec. IV, these eigenmodes fulfill an orthogonality relation and also satisfy the sum rules m_1 and m_3 .

IV. ORTHOGONALITY CONDITION AND SUM RULES

The normal mode solutions of Eq. (42) satisfy obvious orthogonality relations. It is convenient to express these relations in terms of the fields \mathbf{s} and χ . To this end we assume a time dependence of the form

$$A(\mathbf{x}, t) = \sum_{j=1}^{k_{\text{dim}}} \bar{A}^{(j)}(\mathbf{x}) \sin(\omega_j t + \gamma_j), \quad (43)$$

for the field \mathbf{s} , and a time dependence of the form

$$B(\mathbf{x}, t) = \sum_{j=1}^{k_{\text{dim}}} \bar{B}^{(j)}(\mathbf{x}) \cos(\omega_j t + \gamma_j), \quad (44)$$

for the field χ .

From Eq. (35) we may write

$$\int d^3x \delta \chi \left[\nabla \cdot (n_0 \dot{\mathbf{s}}^{(j)}) + \nabla \cdot \left[\frac{n_0}{m} \nabla \chi^{(j)} \right] \right] = 0. \quad (45)$$

Moreover, from Eq. (36) we have

$$\int d^3x \delta \mathbf{s} \cdot \left[n_0 \nabla \dot{\chi}^{(j)} - \frac{\delta E^{(2)}[\mathbf{s}^{(j)}]}{\delta \mathbf{s}^{(j)}} \right] = 0. \quad (46)$$

In Eqs. (45) and (46), $\chi^{(j)}$ and $\mathbf{s}^{(j)}$ stand for the eigensolution of order j , while $\delta\chi$ and $\delta\mathbf{s}$, respectively, are given by the following equations:

$$\delta\chi = \sum_{k=k_{\min}}^{k_{\max}} \delta a_k(t) (r/R)^k Y_{l0}, \quad (47)$$

$$\delta \mathbf{s} = \nabla \left[\sum_{k=k_{\min}}^{k_{\max}} \delta b_k(t) (r/R)^k Y_{l0} \right], \quad (48)$$

where the quantities $\delta a_k(t)$ and $\delta b_k(t)$ are arbitrary.

We consider the symmetric bilinear forms

$$\mathcal{T}^{(2)}[\chi^{(i)}, \chi^{(j)}] \equiv \int d^3x \frac{n_0}{2m} (\nabla \chi^{(i)}) \cdot (\nabla \chi^{(j)}) \quad (49)$$

and

$$\begin{aligned} \mathcal{E}^{(2)}[\dot{\mathbf{s}}^{(i)}, \dot{\mathbf{s}}^{(j)}] &\equiv \int d^3x \left[\frac{\tau_0}{3} [(\nabla \cdot \dot{\mathbf{s}}^{(i)}) (\nabla \cdot \dot{\mathbf{s}}^{(j)}) + \frac{1}{2} (\partial_\alpha \dot{s}_\beta^{(j)} + \partial_\beta \dot{s}_\alpha^{(j)}) (\partial_\alpha \dot{s}_\beta^{(i)} + \partial_\beta \dot{s}_\alpha^{(i)})] + \sum_\sigma a_\sigma \frac{\sigma(\sigma-1)}{2} n_0^\sigma (\nabla \cdot \dot{\mathbf{s}}^{(i)}) (\nabla \cdot \dot{\mathbf{s}}^{(j)}) \right] \\ &+ \frac{e^2}{2} \int d^3x_1 d^3x_2 \frac{[\nabla \cdot (n_0 \dot{\mathbf{s}}^{(i)})]_1 [\nabla \cdot (n_0 \dot{\mathbf{s}}^{(j)})]_2}{|\mathbf{x}_1 - \mathbf{x}_2|}. \end{aligned} \quad (50)$$

Making use of Eq. (45) it may be shown easily that

$$\begin{aligned} \mathcal{T}^{(2)}[\chi^{(i)}, \chi^{(j)}] &= - \int d^3x \chi^{(i)} \nabla \cdot \left[\frac{n_0}{2m} \nabla \chi^{(j)} \right] \\ &= \frac{1}{2} \int d^3x \chi^{(i)} \nabla \cdot (n_0 \dot{\mathbf{s}}^{(j)}) \\ &= - \frac{1}{2} \int d^3x n_0 \dot{\mathbf{s}}^{(j)} \cdot \nabla \chi^{(i)}. \end{aligned} \quad (51)$$

Considering Eq. (46) it is also easy to see that

$$\begin{aligned} \mathcal{E}^{(2)}[\dot{\mathbf{s}}^{(i)}, \dot{\mathbf{s}}^{(j)}] &= \frac{1}{2} \int d^3x \dot{\mathbf{s}}^{(i)} \cdot \frac{\delta E^{(2)}[\dot{\mathbf{s}}^{(j)}]}{\delta \dot{\mathbf{s}}^{(j)}} \\ &= \frac{1}{2} \int d^3x \dot{\mathbf{s}}^{(i)} \cdot (n_0 \nabla \dot{\chi}^{(j)}) \\ &= - \omega_j^2 \int d^3x n_0 \dot{\mathbf{s}}^{(i)} \cdot \nabla \chi^{(j)}. \end{aligned} \quad (52)$$

It then follows that $\int d^3x n_0 \dot{\mathbf{s}}^{(i)} \cdot \nabla \chi^{(j)}$ is zero if $\omega_i \neq \omega_j$. We write $\chi^{(j)}(\mathbf{x}, t) = \bar{\chi}^{(j)}(\mathbf{x}) \beta_j(t)$, and $\mathbf{s}^{(j)}(\mathbf{x}, t) = \bar{\mathbf{s}}^{(j)}(\mathbf{x}) \alpha_j(t)$, and we express the orthogonality relation

as follows:

$$- \frac{1}{2} \int d^3x n_0 \bar{\mathbf{s}}^{(i)} \cdot \nabla \bar{\chi}^{(j)} = \delta_{ij}. \quad (53)$$

We will now show that the present model satisfies the sum rules m_1 and m_3 . Let $\hat{D} = \sum_{i=1}^N D(\mathbf{x}_i)$ be an excitation operator such that $D(\mathbf{x})$ can be expanded in the basis of the eigenfunctions $\bar{\chi}^{(j)}$:

$$D(\mathbf{x}) = \sum_{j=1}^{k_{\dim}} c_j \bar{\chi}^{(j)}(\mathbf{x}) \left[\equiv \sum_{j=1}^{k_{\dim}} c_j \chi^{(j)}(\mathbf{x}, 0) \right]. \quad (54)$$

In Eqs. (43) and (44) all the γ_k 's are taken to be zero, in agreement with the initial condition $\chi(\mathbf{x}, 0) = D$ and $\mathbf{s}(\mathbf{x}, 0) = 0$. From the orthogonality relation it follows that

$$c_j = - \frac{1}{2} \int d^3x n_0 \bar{\mathbf{s}}^{(j)} \cdot \nabla D. \quad (55)$$

We note that the coefficient c_j represents the transition amplitude $\langle j | D | 0 \rangle$. If we now consider Eq. (45) and replace $\delta\chi$ by D , we find

$$\begin{aligned} \mathcal{T}^{(2)}[D] &\equiv \int d^3x \frac{n_0}{2m} (\nabla D) \cdot (\nabla D) = - \int d^3x D \nabla \cdot \left[\frac{n_0}{2m} \nabla D \right] \\ &= - \frac{1}{2} \sum_j c_j \int d^3x D \nabla \cdot \left[\frac{n_0}{m} \nabla \chi^{(j)}(\mathbf{x}, 0) \right] \\ &= \frac{1}{2} \sum_j c_j \int d^3x D \nabla \cdot (n_0 \dot{\mathbf{s}}^{(j)}(\mathbf{x}, 0)) \\ &= - \frac{1}{2} \sum_j c_j \omega_j \int d^3x n_0 \bar{\mathbf{s}}^{(j)} \cdot \nabla D = \sum_{j=1}^{k_{\dim}} c_j^2 \omega_j. \end{aligned} \quad (56)$$

Therefore we have proved that the sum rule m_1 [the energy-weighted sum rule (EWSR)] is fulfilled.

We will now be concerned with the sum rule m_3 (cubic EWSR). We consider $\gamma_k = \pi/2$ in agreement with the initial condition $\chi(\mathbf{x}, 0) = 0$ and $\mathbf{s}(\mathbf{x}, 0) = \nabla D$. We consider the following expansion

$$\nabla D = \sum_{j=1}^{k_{\dim}} d_j \bar{\mathbf{s}}^{(j)} \left[\equiv \sum_{j=1}^{k_{\dim}} d_j \mathbf{s}^{(j)}(\mathbf{x}, 0) \right], \quad (57)$$

where

$$d_j = -\frac{1}{2} \int d^3x n_0(\nabla D) \cdot \nabla \bar{\chi}^{(j)}. \quad (58)$$

Then, from Eq. (46), if we replace δs by ∇D , we find

$$\begin{aligned} E^{(2)}[\nabla D] &= \frac{1}{2} \int d^3x (\nabla D) \cdot \frac{\delta E^{(2)}[\nabla D]}{\delta \nabla D} \\ &= \frac{1}{2} \sum_j d_j \int d^3x (\nabla D) \cdot \frac{\delta E^{(2)}[\mathbf{s}^{(j)}]}{\delta \mathbf{s}^{(j)}} \Bigg|_{t=0} = \frac{1}{2} \sum_j d_j \int d^3x (\nabla D) \cdot (n_0 \nabla \dot{\chi}^{(j)}(\mathbf{x}, 0)) \\ &= -\frac{1}{2} \sum_j d_j d_i \omega_j \int d^3x n_0 \bar{\mathbf{s}}^{(i)} \cdot \nabla \bar{\chi}^{(j)} = \sum_{j=1}^{k_{\text{dim}}} d_j^2 \omega_j. \end{aligned} \quad (59)$$

We now consider Eq. (45) in order to relate the coefficients d_j and c_j . Replacing $\delta \chi$ by D in Eq. (45), one has

$$\int d^3x D \left[\nabla \cdot (n_0 \bar{\mathbf{s}}^{(j)}) + \nabla \cdot \left(\frac{n_0}{m} \nabla \chi^{(j)} \right) \right] = 0. \quad (60)$$

Therefore

$$\omega_j \int d^3x D \nabla \cdot (n_0 \bar{\mathbf{s}}^{(j)}) = - \int d^3x D \nabla \cdot \left(\frac{n_0}{m} \nabla \chi^{(j)} \right). \quad (61)$$

Thus we have $d_j = -m \omega_j c_j$. Finally, we obtain the m_3 sum rule:

$$\sum_{j=1}^{k_{\text{dim}}} \omega_j^3 c_j^2 = \frac{1}{m^2} E^{(2)}[\nabla D]. \quad (62)$$

We remark that Eq. (59) may also be regarded as the m_1 sum rule corresponding to the transition operator $\frac{1}{2}[\mathbf{p} \cdot \nabla D + (\nabla D) \cdot \mathbf{p}]$. Then d_j is the corresponding transition amplitude.

V. NUMERICAL RESULTS

In the method presented in this work, the generator \hat{S} may be written as $\hat{S} = \hat{Q} + \hat{P}$, where \hat{Q} and \hat{P} are Hermitian operators of the types

$$\hat{Q} = \sum_{j=1}^N \chi(\mathbf{x}_j, t) \quad (63)$$

and

$$\hat{P} = \frac{1}{2} \sum_{j=1}^N [\mathbf{p}_j \cdot \mathbf{s}(\mathbf{x}_j, t) + \mathbf{s}(\mathbf{x}_j, t) \cdot \mathbf{p}_j]. \quad (64)$$

We note that in the classical limit the commutator $[Q, H]$ is replaced by the Poisson bracket $i\hbar\{\chi, p^2/2m\} = i(\hbar/m)\mathbf{p} \cdot \nabla \chi$. In the same limit we have $\langle \phi_0 | [\hat{P}, [H, \hat{P}]] | \phi_0 \rangle / \hbar^2 = 2E^{(2)}[\mathbf{s}]$. Therefore we also have

$$\langle \phi_0 | [[H, \hat{Q}], [H, [\hat{Q}, H]]] | \phi_0 \rangle / \hbar^2 = 2E^{(2)}[\nabla \chi] (\hbar/m)^2.$$

Obviously if we expand χ according to Eq. (25), the following relations hold:

$$\langle \phi_0 | [\hat{Q}, [H, \hat{Q}]] | \phi_0 \rangle / \hbar^2 = 2T^{(2)}[\chi] = (1/m) \sum_{kq} A_{kq} a_k a_q,$$

and

$$\langle \phi_0 | [[H, \hat{Q}], [H, [\hat{Q}, H]]] | \phi_0 \rangle / \hbar^2 = (\hbar/m)^2 \sum_{kq} B_{kq} a_k a_q.$$

The eigenvalue equation (42) which we have obtained is equivalent to Eq. (30) of Ref. 18, which was derived from a multidimensional extension of the sum rule approach. We have used a variational method to arrive at the eigenvalue Eq. (42). As we have seen in preceding sections, our method fulfills the sum rules m_1 and m_3 and also gives explicit expressions for the transition density and the transition current. We have seen that k_{min} cannot be less than 2 (1) for $l \neq 1$ ($l=1$). Our method yields the best possible results within the approximation fixed by Eq. (18), if we fix k_{min} at the minimum allowed value and if simultaneously we allow $k_{\text{max}} \rightarrow \infty$. Including all terms of an expansion of the generator \hat{S} in powers of \mathbf{p} in Eq. (18) would lead to the formulation of an exact classical RPA. Less restrictive assumptions for the generator \hat{S} have already been considered,⁶⁻¹² in connection with the analogous nuclear problem.

In recent works,¹⁸⁻²⁰ the energies of the surface and volume plasmons have been calculated for spherical metal clusters using sum-rule arguments and considering the "spill out" of some of the valence electrons outside the jellium. In our present approach, we do not include the gradient terms in the energy functional when treating the equilibrium state. However, we still preserve basic features of quantum systems such as the Pauli principle. Although in the equilibrium state the density of the valence electrons is a step function, our method leads to reliable results because it preserves self-consistency. In the present model, pure surface modes correspond to a transition density proportional to $\delta(R-r)$ which is obtained if $\chi \propto r^l Y_{l0}$. Moreover, it has the advantage of formal and numerical simplicity.

One of the main advantages of this method is the fact that for each choice of k_{max} we obtain not only the most collective state, but also all the first k_{dim} excited states of the system. The energies of the collective states obtained in our method agree with those obtained with sum-rule-based formalisms,²¹ which can give only an estimate of the energy of the most collective state,²⁰ and not the full

TABLE I. For the multipolarity $l=2$, we give the energies of the eigenmodes for different truncation schemes ($2 \leq k_{\text{dim}} \leq 7$), and we compare with the energies of the first seven eigenmodes appearing for $k_{\text{dim}}=15$ in order to study the convergence of the present model. For a test we calculate the lowest eigenvalues of a sodium cluster having 92 atoms.

$\hbar\omega_i$	$k_{\text{dim}}=2$	$k_{\text{dim}}=3$	$k_{\text{dim}}=4$	$k_{\text{dim}}=5$	$k_{\text{dim}}=6$	$k_{\text{dim}}=7$	$k_{\text{dim}}=15$
$\hbar\omega_1$	3.8818	3.8808	3.8806	3.8806	3.8806	3.8806	3.8806
$\hbar\omega_2$	6.8168	6.6064	6.5999	6.5981	6.5981	6.5981	6.5981
$\hbar\omega_3$		8.7820	7.6491	7.6275	7.5982	7.5978	7.5975
$\hbar\omega_4$			11.8016	8.9752	8.9331	8.8047	8.7990
$\hbar\omega_5$				15.7635	10.5694	10.5012	10.1351
$\hbar\omega_6$					20.5634	12.4289	11.5598
$\hbar\omega_7$						26.1378	13.0446

spectrum. In the limit of large clusters ($R \rightarrow \infty$), only the last term in the matrix B_{kq} remains, and we have a semi-infinite system. In this particular case our matrices A_{kq} and B_{kq} agree with the corresponding matrices in Eqs. (36) and (37) of Ref. 18, and our results agree with the results of Ref. 18. Thus, for $l=0$, we obtain the eigenvalue $\omega=\omega_p$, which is k_{dim} -fold degenerate, and for $l>0$ there are the $k_{\text{dim}}-1$ degenerate eigenvalues $\omega=\omega_p$ and we find one nondegenerate eigenvalue $\omega_l=\omega_p\sqrt{l/(2l+1)}$ which is the classical Mie²² frequency and which exhausts the sum rules m_1 and m_3 .

The number of eigenfrequencies ω_j and the number of eigenfields ($\chi^{(j)}, s^{(j)}$) is equal to k_{dim} and depends therefore on the value k_{max} for which we truncate Eqs. (24) and (25). As an example, in Table I for different values of k_{max} ($k_{\text{min}}=2$), we give the energies of the eigenmodes appearing for $l=2$. In principle, k_{max} is arbitrary, and the best results would be obtained when we let $k_{\text{max}} \rightarrow \infty$. Each time we increase k_{max} by one unit we are adding a term proportional to $(r/R)^{k_{\text{max}}}$ in expansions (24) and (25), and as a consequence a new normal mode appears which has the particularity of being the eigenmode with the highest energy. When increasing k_{max} , the energies of the lower eigenmodes show up to be very stable with respect to the values they possessed in the previous truncation scheme. We can also conclude from Table I that the convergence is faster for the lower modes, which are, therefore, especially stable, being independent of the particular truncation scheme.

As quoted above, a variational method of this kind was first applied in nuclear physics, for the description of the giant resonances.⁴ Therefore, as a test of the present method, which uses a polynomial expansion of the variational fields, we began by considering the nuclear case. Considering $k_{\text{dim}}=10$ we have been able to reproduce,

with excellent accuracy, the results presented in Refs. 4 and 7, which also use a ‘‘square-well’’ equilibrium density.

When treating the metal clusters, where we are mainly interested in the energy spectrum of the excited states, we chose an effective interaction of the form

$$V_{\text{eff}} = \int d^3x (a_1 n + a_2 n^2 + a_3 n^3), \quad (65)$$

where the set of effective parameters a_1 , a_2 , and a_3 is chosen in such a way that the binding energy E/N , the jellium density n_0 , and the bulk modulus \mathcal{B} have the known experimental values of a homogeneous system of atoms of the element considered. These parameters have been calculated providing that self-consistency, as expressed by Eq. (13), is satisfied. For E/N we have taken the value obtained by adding the cohesion energy (energy necessary for sublimation) to the ionization energy.^{23,24} Further, we note that the matrices A_{kq} and B_{kq} depend only on \mathcal{B} , n_0 , and τ_0 , and therefore we would obtain the same energies of the eigenmodes if these quantities remained constant but E/N was replaced by another value and new force parameters were calculated. The set of parameters we have used is given, for each cluster, in Table II.

An interesting aspect is the N dependence of the energies of the eigenmodes. From Eqs. (42), (31), and (32), we can easily see that, if it were not for the last term in Eq. (32), which is proportional to R , ω would be proportional to $N^{-1/3}$, which is a well-known behavior of the giant resonances in nuclei. In any case, for N smaller than a certain value, the last term in Eq. (32) can be neglected when compared to the others, and a behavior close to $\omega \propto N^{-1/3}$ shows up in the energies of the eigenmodes for all multiplicities, including $l=0$. This can be clearly observed for sodium (Figs. 1 and 4), aluminum (Fig. 2), and

TABLE II. Parameters of the effective force a_1 , a_2 , and a_3 , binding energy E/N , electronic density n_0 , and bulk modulus \mathcal{B} for sodium, aluminum, and silver.

	a_1 [eV \AA^{-3}]	a_2 [eV \AA^{-6}]	a_3 [eV \AA^{-9}]	E/N [eV]	n_0 [\AA^{-3}]	\mathcal{B} [eV]
Na	-5.8348×10^0	-1.3317×10^2	1.6429×10^3	-6.2669	2.5435×10^{-2}	4.3372×10^{-2}
Al	-1.9147×10^1	-4.8474×10^1	6.2751×10^1	-18.8642	1.8065×10^{-1}	4.5925×10^{-1}
K	-4.7922×10^0	-1.9685×10^2	5.0933×10^3	-5.2811	1.3277×10^{-2}	2.0222×10^{-2}
Ag	-5.8043×10^0	-2.3660×10^2	1.6978×10^3	-10.5381	5.8620×10^{-2}	6.4100×10^{-1}

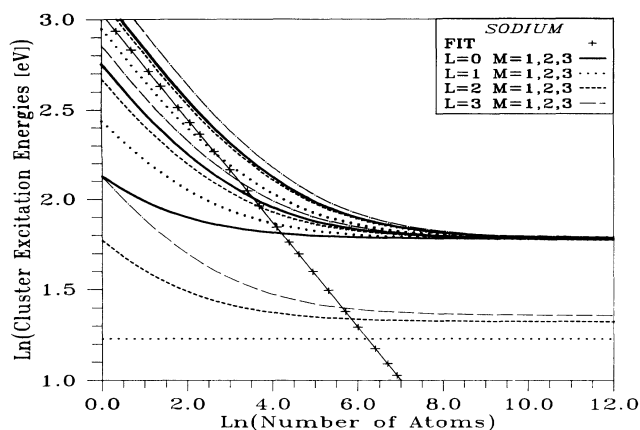


FIG. 1. Natural logarithm of the cluster excitation energy vs the natural logarithm of the number of atoms of the cluster, for sodium, for angular momenta $0 \leq l \leq 3$ for the first three eigenstates of each multiplicity. A fit ($20.6N^{-0.315}$ eV) to the initial slope of the energy variation of these low-lying modes is also shown, as a solid line with crosses. In all the figures to come, L stands for the angular momentum, and M for the order of the eigenmode, being the eigenmodes ordered from the lowest ($M=1$) to the highest-energy eigenvalues.

silver (Fig. 3). For the pictures in log scale where the linear behavior is very clear, as well as for the monopole energies, a fit was made to show how close we are to the $N^{-1/3}$ behavior. For sodium, for the third eigenmodes of the four lowest angular momenta, the fit (straight line with crosses) reveals a $N^{-0.315}$ behavior up to about 200 atoms for sodium.

For higher modes and higher angular momenta, this linear behavior is followed for even larger clusters (up to many thousands of atoms), as we can see from Fig. 3, where the fit to the higher-lying states shows a $N^{-0.33}$ behavior, already closely approaching the $N^{-1/3}$ dependence of the self-bound nuclear systems.

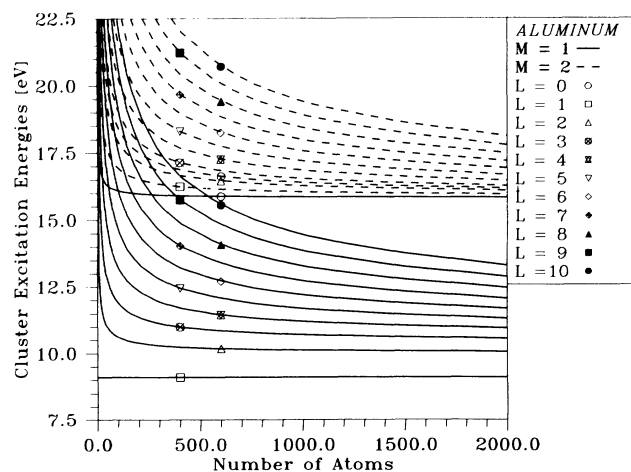


FIG. 2. Cluster excitation energy vs the number of atoms of the cluster, for aluminum, for angular momenta $0 \leq l \leq 10$ for the first two eigenstates of each multiplicity. The solid lines stand for the first (lowest-lying) mode, and the dashed lines for the second.

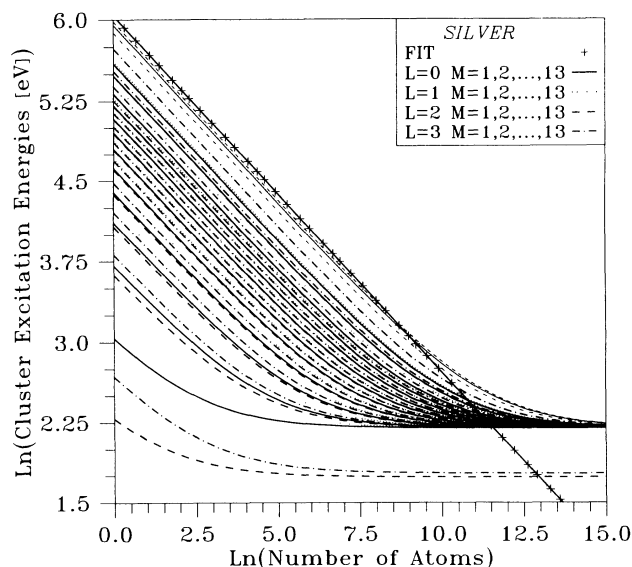


FIG. 3. Natural logarithm of the excitation energy vs the natural logarithm of the number of atoms of the cluster, for silver, for angular momenta $0 \leq l \leq 3$ for the first 13 eigenstates of each multiplicity. A fit ($419.9N^{-0.33}$ eV) to the initial slope of the energy variation of the higher-lying modes is also shown, as a solid line with crosses.

We now consider Fig. 4, which represents the energies of the nine lowest monopole eigenmodes as a function of the number of atoms of the cluster. The collective (first) state has a behavior close to the expected dependence of $\sqrt{m_3/m_1}$, as a function of N and the higher modes also show a similar behavior. We also see that these curves decrease when N increases. As we have pointed out, this behavior is in agreement with that expected for giant resonances in nuclear physics. This is different from the behavior displayed in Figs. 4–6 of Ref. 20, and Fig. 3 of Ref. 18, which, for the special case of $l=0$, show an increase of $\sqrt{m_3/m_1}$ when N increases, until the value of the volume plasmon is reached for $N \rightarrow \infty$.

As we have shown in Sec. IV, the present model satisfies the m_1 and m_3 sum rules, as long as we consider

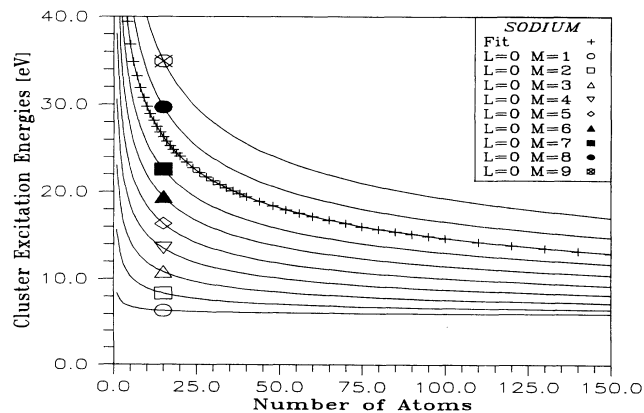


FIG. 4. Excitation energies of the sodium cluster for the monopole, for the nine first (lowest) eigenstates, vs the number of atoms of the cluster. A fit of the form ($60.3N^{-0.31}$ eV) is also shown as a solid line with crosses.

an operator which may be expressed as

$$D(\mathbf{x}) = \sum_{k=k_{\min}}^{k_{\max}} v_k r^k Y_{l0} . \quad (66)$$

We then have $m_1 = T^{(2)}[D]$ and $m_3 = E^{(2)}[\nabla D]/m^2$, where $T^{(2)}[D]$ and $E^{(2)}[\nabla D]$ are given by Eqs. (29) and (30), if we replace a_k and b_k by $v_k R^k$. In particular, we consider the operators

$$D(\mathbf{x}) = r^2 \text{ for } l=0, \text{ and } D(\mathbf{x}) = r^l Y_{l0} \text{ for } l > 0 . \quad (67)$$

Then for $D(\mathbf{x}) = r^2$ we have

$$m_1 = \frac{8\pi n_0(0)R^5}{5m} \quad (68)$$

and

$$m_3 = \frac{24\pi R^3 \mathcal{B}}{m^2} + \frac{8\pi n_0(0)R^5}{5m} \omega_p^2 , \quad (69)$$

and for $D(\mathbf{x}) = r^l Y_{l0}$ we have

$$m_1 = \frac{n_0(0)}{2m} l R^{2l+1} \quad (70)$$

and

$$m_3 = \frac{2\tau_0(0)R^{2l-1}}{3m^2} l(l-1)(2l+1) + \frac{n_0(0)\omega_p^2 R^{2l+1}l^2}{2m(2l+1)} . \quad (71)$$

We shall now focus on the sodium clusters. The energies of the three lowest eigenmodes are given in Fig. 1, up to $l=3$. In Table III we present these energies up to $l=5$, for $N=92$, together with the percentages of m_1 and m_3 sum rules [for the excitation operators given by Eq. (67)] exhausted by each state. Further, in Table IV we give the quantities $\sqrt{m_3/m_1}$ which indicate the position of an eigenmode that exhausts completely both m_1 and m_3 sum rules. If the mode only partially exhausts these sum rules (as it is usually the case), then $\sqrt{m_3/m_1}$ gives an upper bound to the energy of this collective mode. We can see from Table III that, for $l=1$, the only state which exhausts 100% of the EWSR and the cubic EWSR, the energy of the state given in Table III, coincides with the value of $\sqrt{m_3/m_1}$, given in Table IV. For all the other states, which only partially exhaust the sum rules, their energies lie somewhat below the (upper bound) value of $\sqrt{m_3/m_1}$, as they should.

For large values of N , the first mode of each multipolarity (except $l=0$) converge for values close to the surface plasmon, defined by the first dipole mode; in other words, they converge to the Mie limit of each multipolarity. The higher modes converge to the bulk volume plasmon, defined by the first monopole mode, as can be seen in the log plots for sodium (Fig. 1) and silver (Fig. 3), and also in the linear plot for aluminum (Fig. 2), where the first (solid line) and second (dashed line) modes for the first ten angular momenta are shown. The collective 1_1^- , which is constant with respect to the number of atoms, is the lowest Mie limit. The other collective states

TABLE III. Picking up some of the results for a sodium cluster of 92 atoms, for each multipolarity (first column) we list the excitation energies (second column), the exhausted percentage of the m_1 sum rule (third column), and the exhausted percentage of the m_3 sum rule (fourth column). An equilibrium distribution function of the Fermi type [Eq. (9)], satisfying the equilibrium condition (13) was considered.

l_i^π	$\hbar\omega_i$ [eV]	m_1 [%]	m_3 [%]
0_1^+	6.0666	97.662	96.568
0_2^+	6.7397	1.837 6	2.242 6
0_3^+	7.7130	0.318 22	0.508 63
1_1^-	3.4191	100	100
1_2^-	6.3078	0.0	0.0
1_3^-	7.1528	0.0	0.0
2_1^+	3.8806	99.947	99.751
2_2^+	6.5981	0.030 618	0.088 343
2_3^+	7.5975	0.011 023	0.042 172
3_1^-	4.2232	99.735	98.832
3_2^-	6.9310	0.156 46	0.417 60
3_3^-	8.0675	0.054 262	0.196 21
4_1^+	4.5675	99.340	97.247
4_2^+	7.3002	0.393 22	0.983 34
4_3^+	8.5579	0.133 03	0.457 19
5_1^-	4.9345	98.777	95.180
5_2^-	7.7001	0.730 92	1.714 9
5_3^-	9.0647	0.243 47	0.791 71

($2_1^+, 3_1^-, 4_1^+, \dots$, except the 0_1^+) converge to their Mie limit, namely $1/\sqrt{2}\omega_{0_1^+}(N \rightarrow \infty) = 1/\sqrt{2}\omega_p \leq \omega_{\text{Mie}} \leq \omega_p/\sqrt{3} = \omega_{1_1^-}$.

Our model, being a semiclassical one, is expected to give its best description of the spectra for very large clusters. However, experimental results for neutral clusters are only available for the smallest clusters, and for the $l=1$ state, mostly for alkaline metals.²⁵⁻³³ For potassium ions, there are some results for clusters up to some hundreds of atoms.^{34,35} From this reference we extract, for K_{90}^+ , $E^{\text{exp}} = 2.05$ eV. The result of our work is $E = 2.47$ eV. This is in fair agreement, not only with the data, if we consider that we calculate a neutral cluster and further corrections should be introduced in order to describe an ion cluster,³⁵ but also with other theoretical calculations quoted in Ref. 35, based on the works of

TABLE IV. For the multiplicities listed in the first column, the quantities $(m_3/m_1)^{1/2}$ are calculated in the second column, where m_1 and m_3 are the energy-weighted and cubic-energy-weighted sums calculated for the distribution function (9) and the excitation operators (67), respectively.

l^π	$\hbar\sqrt{m_3/m_1}$
0^+	6.1108
1^-	3.4191
2^+	3.8844
3^-	4.2425
4^+	4.6164
5^-	5.0269

TABLE V. Calculated (this work with $R \rightarrow \infty$) and experimental (Ref. 41) energies of the volume and surface plasmons for sodium, potassium, aluminum, and silver.

Element	$\hbar\omega_p$ (eV) this work	$\hbar\omega_p$ (eV) experimental	$\hbar\omega_p/\sqrt{2}$ (eV) this work	$\hbar\omega_s$ (eV) experimental
N	5.92	5.72	4.19	4.28
K	4.28	3.72	3.03	3.11
Al	15.78	15.0	11.16	11.19
Ag	8.99	3.78	6.36	6.35

Kresin^{36,37} and Bertsch.³⁸

Moreover, we see from our results that for simple metal clusters (Na, K, Al) we are within 0.1% of the classical result only when the number of atoms of the cluster $N > 10^4$ for the volume plasmon, and only when $N > 10^5$ for Ag. Therefore, for $N=900$, we are still far from the region where our semiclassical model can give its best description of data.

Up to now, our best testing field has been the infinite radius limit, where we can compare our results for the volume modes to the bulk plasmon, whose location is experimentally well established for a large number of metals.^{39,40} In Table V, the results of this work are shown, as well as the experimental results for the volume and surface plasmons for the bulk metal, and we can see that we have, in general, a very good agreement in this limit. In some cases, specific structure effects which are not embodied in this model cause the cluster energies to deviate from the expected semiclassical values, as is the case for silver.⁴¹ Obviously, for a plane surface we should have $l \rightarrow \infty$ (in order to have a finite wavelength). It is then clear that in the limit of a plane surface, when $R \rightarrow \infty$ and $l \rightarrow \infty$, we have $E_3 \equiv \sqrt{m_3/m_1} = \omega_p/\sqrt{2}$, this being the energy associated with the surface mode in this limit.⁴² In Table V we compare $\omega_p/\sqrt{2}$ with the experimental values for the energy of the surface plasmon.

We consider now the results for the different multiplicities. We present the results in terms of radial functions j_{\pm} defined by

$$\mathbf{j}(\mathbf{x}) = j_+(r)\mathbf{Y}_{l+10} + j_-(r)\mathbf{Y}_{l-10}, \quad (72)$$

where $\mathbf{Y}_{l\pm 10}$ stand for the vector spherical harmonics.

Monopole modes ($l=0^+$) are purely longitudinal modes. In this case all eigenmodes are volume modes in the sense that the transition density is nonzero (or close to it) inside the cluster. In Fig. 5 we present the flow field corresponding to the eigenmodes 0_1^+ and 0_2^+ . The j_- component of the current is proportional to \sqrt{l} , being therefore zero for $l=0$. The transition density $\delta\rho$ for $M=2$ (second mode) presents a further node in regard to $M=1$ (lowest-lying mode), as expected, both being peaked at the cluster interior. In all pictures concerning currents and densities, for the sake of clarity, we scaled the smaller quantities by a suitable factor, as shown in each picture.

The lowest 1^- mode occurs at a finite energy ($\hbar\omega_{1^-} = 3.4191$ eV) and exhausts the sum rule m_1 and m_3 . If it were not for the Coulomb term which is respon-

sible for the appearance of the last term in Eq. (32), this state would represent a uniform translation, which occurs at zero energy, known in nuclear physics as a "spurious state." In the present case this eigenmode is associated with a translation of the valence electrons vs the jellium, breaking this former translational symmetry and leading, therefore, to this eigenmode acquiring a nonzero energy. The velocity potential for this eigenmode is $\chi \propto z$. In Fig. 6 we show the transition density and the current corresponding to the second dipole excited state 1_2^- .

For $l \geq 2$ ($l=2^+, 3^-, 4^+, 5^-, \dots$) the largest fraction of the m_1 sum is exhausted by the lowest eigenmode for each multipolarity which corresponds to a surface mode, because these modes show a small amount of compression in the cluster interior. In Figs. 7 and 8 we plot the flow fields corresponding to the eigenmodes 2_1^+ and 2_2^+ .

The j_+ component of the current and the transition density of the 2_1^+ state, differing from zero only close to the surface, and peaking at the surface, show the deviation of the actual flow from the $r^l Y_{10}$ behavior. The same can be observed in the slight bending of the j_- component of the current close to the surface, since these quantities are connected through the continuity equation.

We also see that, as we consider larger values of l , the fraction of the sum rules exhausted by the surface mode decreases. This might point to the fact that as l increases the strength is more distributed.

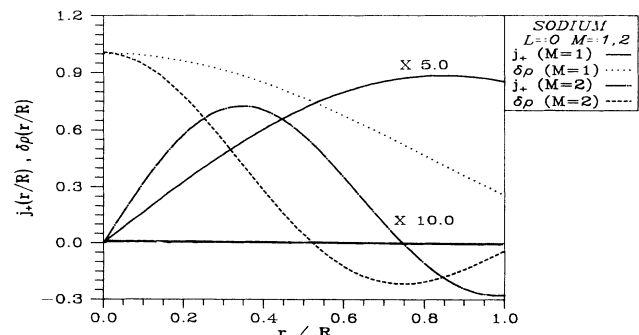


FIG. 5. For a sodium cluster of 92 atoms (radius $R=9.5226$ Å), we show, for the monopole, the transition density (dotted curve for 0_1^+ , and dashed curve for 0_2^+) and j_+ component of the current (solid curve for 0_1^+ and solid-dotted curve for 0_2^+) for the first (lowest) and second eigenmodes of the system. Since in a fluid-dynamical formalism we have a free overall multiplicative factor in the currents and densities, we normalized the larger to unity and, for the sake of clarity, scaled the smaller components as indicated in the figures.

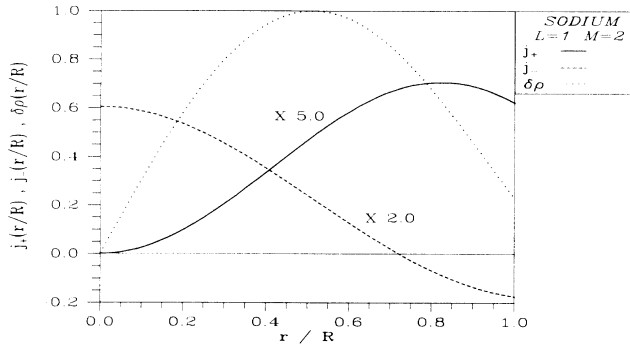


FIG. 6. For a sodium cluster of 92 atoms, we show, for the dipole, the transition density (dotted curve) and the j_{\pm} components of the current (solid curve for j_{+} , and dashed curve for j_{-}) for the second eigenmode of the system.

We could also study the relative importance of the compression character of any of these modes, just by using an operator of the form $r^{l+\alpha}Y_{l0}$ or, generally, $\sum_{\alpha} \gamma_{\alpha} r^{l+\alpha} Y_{l0}$, together with the appropriate sum rules, a method already used in nuclear physics to determine the location, concentration, and strength of compression modes.⁴³

We have seen that for each multipolarity the energy of the lowest eigenmode is rather close to $E_3 = \hbar \sqrt{m_3/m_1}$, due to the fact that this mode exhausts most of the two sum rules. For this reason it is instructive to write the expressions m_3/m_1 for the operators $D(\mathbf{x}) = r^2$, which suits a monopolar excitation, and which in the limit of large clusters lead to the bulk volume plasmon, and $D(\mathbf{x}) = r^l Y_{l0}$, suiting a general multipolar excitation. We have the ratios

$$E_3(l=0) \equiv \left[\frac{m_3[r^2]}{m_1[r^2]} \right]^{1/2} = \left[\frac{15\mathcal{B}}{mn_0(0)R^2} + \omega_p^2 \right]^{1/2}, \quad (73)$$

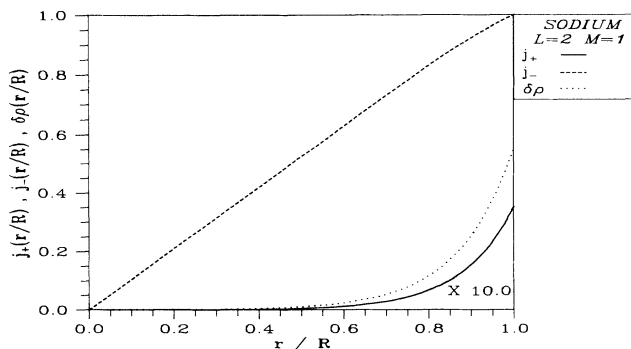


FIG. 7. For a sodium cluster of 92 atoms, we show, for the quadrupole, the transition density (dotted curve) and the j_{\pm} components of the current (solid curve for j_{+} , and dashed curve for j_{-}) for the first (lowest) eigenmode of the system.

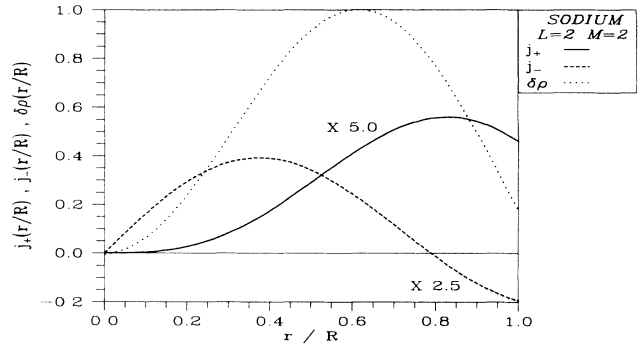


FIG. 8. For a sodium cluster of 92 atoms, we show, for the quadrupole, the transition density (dotted line) and the j_{\pm} components of the current (solid curve for j_{+} , and dashed curve for j_{-}) for the second eigenmode of the system.

and

$$E_3(l \neq 0) \equiv \left[\frac{m_3[r^l Y_{l0}]}{m_1[r^l Y_{l0}]} \right]^{1/2} = \left[\frac{4}{3mR^2} \frac{\langle t \rangle}{N} (l-1)(2l+1) + \frac{l}{2l+1} \omega_p^2 \right]^{1/2}. \quad (74)$$

If it were not for the ω_p^2 term which appears in Eqs. (73) and (74), the energies would be proportional to $N^{-1/3}$, and we would have the same results as in nuclear physics,⁷ with the energies exhibiting the same N dependence characteristic of the nuclear giant resonances. In Eq. (74) $\langle t \rangle = \Omega \tau_0$ stands for the total kinetic energy in the equilibrium state. Finally we note that in our formulation it becomes explicit that the energy of the collective monopole depends basically on the bulk modulus \mathcal{B} of the system, and on its size R (plus the bulk-plasmon term), and that the other multipolar energies depend basically on the kinetic-energy content of the system $\langle t \rangle$ and on its size R (plus the Mie term).

VI. CONCLUSIONS

The fluid-dynamical model presented here is able to describe the main features of cluster excitations, giving a good prediction of the excited energies, especially for larger clusters, where microscopic calculations are nearly impossible, and semiclassical aspects play a dominant role. It has the advantage of being able to handle clusters with an arbitrarily large number of atoms, not only yielding the excitation energies and the exhausted fractions of the main sum rules, but also providing a deeper insight into the transitions, through the transition densities and currents.

No doubt that sum-rule-based methods²¹ are useful tools to investigate collective dynamical properties of many-body systems, but a fluid-dynamical formulation, such as the one presented here, allows us to access problems which are beyond the scope of a pure sum-rule approach.

As shown above the present model satisfies the single-energy-weighted sum rule m_1 , and the cubic-energy-weighted sum rule m_3 . The fulfillment of the sum rules acts as a further check of our results.

We have derived equations of motion for the collective variables by means of a dynamical variational method,^{4,8,15} obtained from the quantum-mechanical action principle. Our method involves the expansion of the generator of $S = Q + P$ in powers of the momentum, and we have considered in such an expansion the simplest scheme which is given by Eq. (18). In Refs. 18 and 19 a static Rayleigh-Ritz-like variational principle was formulated and applied to an expansion of the generator Q in powers of the momentum. Both methods lead to similar sets of equations. This is not surprising since the quantal action principle and the quantal Rayleigh-Ritz variational principle provide equivalent descriptions of static states.

The present variational scheme is directly related to the hierarchy of equations derived in Ref. 15 for an homogeneous system, where a variational scheme was considered in order to obtain approximate solutions to the Vlasov equation. Such a scheme is based on the expansion of the generator S in powers of the momentum \mathbf{p} . Considering a finite number of terms in such an expansion, a closed set of equations is obtained which leads to approximate solutions of the Vlasov equation, and which are in good agreement with the exact solution known for a homogeneous system. The method which we have been studying corresponds to the simplest scheme of Ref. 15, where the generator S only has a term of order zero and a linear term in the momentum \mathbf{p} .

Effective δ interactions have been introduced in order to adjust physical properties of a semiclassical treatment.

We remark that Eq. (42), which expresses the eigenvalue problem and therefore determines the vibrational modes of the valence electrons, depends only on physical quantities such as the equilibrium density ρ_0 , the kinetic-energy density τ_0 , and the bulk compression modulus \mathcal{B} .

We have shown that the fluid-dynamical model developed in this work can be extended easily to a large class of systems such as metal clusters, in which the Coulomb interaction plays a relevant role. Other fluid-dynamical models⁶⁻¹² have been considered previously for finite systems. However, the present model, due to its parametrization, provides a simpler description of the collective dynamics when long-range forces are present. In a forthcoming publication, in preparation, applications to other systems will be made.

The results presented here are in good agreement with the available experimental data, in spite of referring to a step-function density. This shortcoming means that we are not able to take into account some of the surface effects. In a further paper we shall extend the model, allowing for a smooth ground-state density profile, which will allow for the electronic "spill out."

ACKNOWLEDGMENTS

The authors would like to acknowledge discussions with N. Barberán. One of us (R.H.) would like to acknowledge the kind hospitality of the Departamento de Física da Universidade de Coimbra during the accomplishment of this work. This work benefited from computation facilities offered by the Instituto Nacional de Investigação Científica, Lisboa and by the Deutsche Gesellschaft für Technische Zusammenarbeit (GTZ) GmbH.

*Permanent address: Instituto de Física, Universidade Federal do Rio de Janeiro, 21945-Ilha do Fundão, Rio de Janeiro, Brazil.

¹W. A. de Heer, W. D. Knight, M. Y. Chou, and M. L. Cohen, *Solid State Phys.* **40**, 93 (1987).

²*Physics and Chemistry of Small Clusters*, Vol. 158 of *NATO Advanced Study Institute, Series B: Physics*, edited by P. Jena, B. Rao, and S. N. Khanna (Plenum, New York, 1987).

³V. V. Kresin, *Phys. Rep.* **220**, 1 (1992).

⁴K. Andō and S. Nishizaki, *Prog. Theor. Phys.* **68**, 1196 (1982).

⁵J. da Providência, Jr. and N. Barberán, *Phys. Rev. B* **45**, 6935 (1992); J. da Providência, Jr., *Solid State Commun.* **86**, 573 (1993).

⁶G. Eckart, G. Holzwarth, and J. P. da Providência, *Nucl. Phys. A* **364**, 1 (1981).

⁷J. P. da Providência, *Prog. Theor. Phys.* **75**, 862 (1986).

⁸J. P. da Providência and G. Holzwarth, *Nucl. Phys. A* **398**, 59 (1983); J. P. da Providência, *J. Phys. G* **13**, 783 (1987).

⁹J. da Providência, Jr., *Nucl. Phys. A* **510**, 322 (1990).

¹⁰J. P. da Providência and G. Holzwarth, *Nucl. Phys. A* **439**, 477 (1985).

¹¹J. P. da Providência, *J. Phys. G* **13**, 481 (1987).

¹²L. Brito and C. Providência, *Phys. Rev. C* **32**, 2049 (1985); J. da Providência, Jr., L. Brito, and C. Providência, *Nuovo Cimento* **87**, 248 (1985).

¹³J. da Providência, Jr., *Nucl. Phys. A* **523**, 247 (1991).

¹⁴S. Nishizaki and K. Andō, *Prog. Theor. Phys.* **73**, 889 (1985).

¹⁵J. P. da Providência, *Nucl. Phys. A* **489**, 111 (1988).

¹⁶W. Ekaradt, *Phys. Rev. B* **31**, 6360 (1985), and references therein.

¹⁷C. Yannouleas, E. Vigezzi, and R. Broglia, *Phys. Rev. B* **47**, 9849 (1993).

¹⁸M. Brack, *Phys. Rev. B* **39**, 3533 (1989).

¹⁹P.-G. Reinhard, M. Brack, and O. Genzken, *Phys. Rev. A* **41**, 5568 (1990).

²⁰L. Serra, F. Garcias, M. Barranco, J. Navarro, C. Balbàs, and A. Mañanes, *Phys. Rev. B* **39**, 8247 (1989).

²¹E. R. Marshalek and J. da Providência, *Phys. Rev. C* **7**, 2281 (1973).

²²G. Mie, *Ann. Phys. (Leipzig)* **25**, 377 (1908).

²³J. Emsley, *The Elements* (Clarendon, Oxford, 1991).

²⁴K. A. Gschneider, in *Solid State Physics*, edited by F. Seitz and D. Turnbull (Academic, New York, 1964).

²⁵K. Selby, M. Vollmer, J. Masui, W. A. de Heer, and W. D. Knight, *Phys. Rev. B* **40**, 5417 (1989).

²⁶C. R. C. Wang, S. Pollack, D. Cameron, and M. Kappes, *J. Chem. Phys.* **93**, 3787 (1990).

²⁷W. A. de Heer, K. Selby, V. Kresin, J. Masui, M. Vollmer, A. Chatelain, and W. D. Knight, *Phys. Rev. Lett.* **59**, 1805 (1987).

²⁸C. R. C. Wang, S. Pollack, T. A. Dahlseid, G. M. Koretsky, and M. Kappes, *J. Chem. Phys.* **96**, 7931 (1992).

- ²⁹K. Selby, V. Kresin, J. Masui, M. Vollmer, W. A. de Heer, A. Scheidemann, and W. D. Knight, *Phys. Rev. B* **43**, 4565 (1991).
- ³⁰C. R. C. Wang, S. Pollack, J. Hunter, G. Alameddin, T. Hoover, D. Cameron, S. Liu, and M. Kappes, *Z. Phys. D* **19**, 13 (1991).
- ³¹H. Fallgren and T. P. Martin, *Chem. Phys. Lett.* **168**, 233 (1990).
- ³²H. Fallgren, K. M. Brown, and T. P. Martin, *Z. Phys. D* **19**, 81 (1991).
- ³³M. Broyer, J. Chevaleyre, and Ph. Dugourd, *Phys. Rev. A* **42**, 6954 (1990).
- ³⁴C. Bréchnignac, Ph. Cahuzac, F. Carlier, and J. Leygnier, *Chem. Phys. Lett.* **164**, 433 (1989).
- ³⁵C. Bréchnignac, Ph. Cahuzac, N. Kebaili, J. Leygnier, and A. Sarfati, *Phys. Rev. Lett.* **68**, 3916 (1992).
- ³⁶V. Kresin, *Phys. Rev. B* **39**, 3042 (1989).
- ³⁷V. Kresin, *Phys. Rev. B* **40**, 12 508 (1989).
- ³⁸G. Bertsch, *Comput. Phys. Commun.* **60**, 247 (1990).
- ³⁹H. Raether, *Excitation of Plasmons and Interband Transitions by Electrons* (Springer-Verlag, Heidelberg, 1980).
- ⁴⁰K. D. Tsuei, E. W. Plummer, A. Liebsch, E. Pehlke, K. Kempa, and P. Bakshi, *Surf. Sci.* **247**, 302 (1991).
- ⁴¹A. Liebsch, *Phys. Rev. Lett.* **71**, 145 (1993).
- ⁴²K. D. Tsuei, E. W. Plummer, A. Liebsch, K. Kempa, and P. Bakshi, *Phys. Rev. Lett.* **64**, 44 (1990).
- ⁴³R. de Haro, S. Krewald, and J. Speth, *Phys. Rev. C* **26**, 1649 (1982).